

# RESEARCH ON WIND PERFORMANCE AND FIELD EXPERIMENT OF LARGE SCALE COMPLEX SURFACE SPACE TRUSS WITH STEEL PIPE

XIULI WANG<sup>1,2</sup>, YONGHONG RAN<sup>1,2</sup>, HUVUE ZHANG<sup>1,2</sup>, and YANPENG ZHU<sup>1,2</sup>

<sup>1</sup>*School of Civil Engineering, Lanzhou University of Technology, Lanzhou, China*

<sup>2</sup>*Western Center of Disaster Mitigation in Civil Engineering, Lanzhou University of Technology, Lanzhou, China*

The wind-induced performance response of large-span truss curved roofs is extremely complex and changes obviously under wind load. This paper has taken the large-span steel roof of *Liu Zhaike* highway toll station as an example to analyze by both numerical simulations and field tests of responses of the steel canopy under wind load. In this case, simulated analysis results using finite element software were calibrated and verified by the field test results. In addition, a new method of large structure field testing was proposed which obtained the internal force and displacement of the canopy structure. Moreover, this paper analyzed and determined the actual stress state of the rectangular pipe truss. Finally, the safety condition of the roof was evaluated based on the monitoring data and the simulation of the finite element model. And the analysis methods provides references for similar engineering field tests, as well as guidance for the operation and maintenance for this project.

*Keywords:* Rectangular steel tube truss, Numerical wind tunnel, Coefficient of wind pressure, Shape factor, Field test.

## 1 INTRODUCTION

Large-span structures are attributed to wind-induced sensitive ones, and the wind load tends to be the main control load of the structural design (Xiang 1997). For example, *Zhengzhou* stadium suffered from disaster caused by a windstorm in 2003, with more than 4000 m<sup>2</sup> cantilevered roof whipped by strong winds, and the direct loss of about ¥240,000 (Pan 2008). Although the structural wind resistance analysis of the numerical wind tunnel method has been carried out for such structures (Ma *et al.* 2007), and the computer finite element technology is employed to analyze precisely various stress conditions of structures, there may be a great deviation between the calculated results and the actual force of the structure due to the errors in load assumption (Chen *et al.* 2010, Shen and Wu 2010). Therefore, it is of great theoretical significance and practical value to carry out field experiments under special wind load conditions of large-scale projects. However, the field load tests of large space structures are few at home and abroad (Zhou *et al.* 2012). Taking the large roof structure of *Liu Zhaike* expressway toll station as an example, the numerical simulation of wind tunnel and field load test are carried out to study the structural response of rectangular steel truss with space-curved surface under wind load. Meanwhile, a loading method for field test of large structure is presented, and the results of numerical simulation and field test are compared and analyzed.

## 2 PROJECT OVERVIEW

The new toll station of *Liu Zhaike* is located in *Wuhe* Township of *Jingyuan* County, *Gansu*, China, which is also the juncture of *Gansu* and *Ningxia*. The average altitude is 1693 m, with extensive terrain and strong wind. The average maximum wind speed is 1.8 m/s, and the instantaneous maximum wind speed reaches 23.2 m/s over the years. The region is also full of windy days, and the average annual number of days with wind speed exceeding 5 m/s reaches 160 days. Therefore, wind loads are the main factor to be considered for this structure. The total height of the new toll station roof in *Liu Zhaike* is 23.8 m, with the width of 21 m, and the total length is 112.4 m, and the projected area of the building 2360.40 m<sup>2</sup>. The toll booth is made up of two parts: steel structure and membrane structure. And the steel structure is made up of space plane rectangular steel tube truss structure, the whole building surface formed by vertical and horizontal crossing (Figure 1).



Figure 1. Construction site.

## 3 SIMULATION OF NUMERICAL WIND TUNNEL

### 3.1 Computational Model

#### 3.1.1 Wind direction

The geometric entity model is shown in Figure 2. Since the toll station is a biaxial symmetric structure, the wind load under 7 wind directions (0°, 15°, 30°, 45°, 60°, 75° and 90°) are chosen as the simulated condition (Figure 3). Among them, the 0° wind direction is the wind load parallel to the north-south direction, with the smallest windward area; The 90° wind direction is the wind load parallel to the east-west direction, with the biggest windward area.

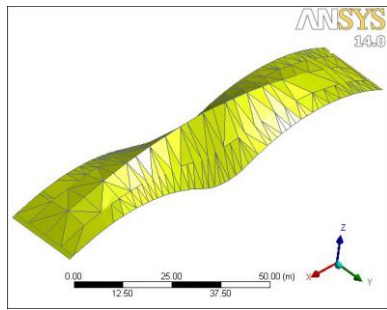


Figure 2. Geometry model of the toll station.

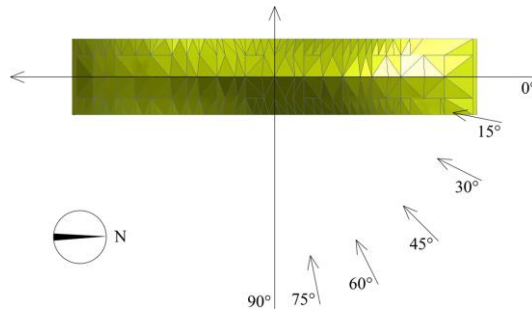


Figure 3. Wind direction diagram.

#### 3.1.3 Computing watershed model

Dimension of computing watershed in the structure refers to the design parameters of large span structures in reference (Li 2013).  $L1$ , advanced position of computing watershed, is 190 meters according to dimension of building surface ( $l_x \times l_y \times l_z = 21 \times 112.4 \times 23.8 \text{ m}$ ), and  $L2$ , as the

backward position of computing watershed, is 285 m, with its width  $B$  450 m. The dimension of computing watershed is  $B \times L \times H = 450\text{m} \times 500\text{m} \times 238\text{m}$ .

### 3.1.4 Boundary condition

Entrance boundary condition: Surface roughness of the structure is class B, and basic wind pressure  $\omega_0 = 0.45\text{kN} \cdot \text{m}^{-2}$ , reappearing period 50 years. The average wind speed at the standard reference height 10 m can be calculated as:  $u_0 = 28.77\text{m} \cdot \text{s}^{-1}$ . The characteristics of free-stream turbulence are defined by the method of directly giving the turbulent kinetic energy  $k$  and turbulent dissipation rate  $\varepsilon$ .

Exit boundary condition: Boundary conditions of building surface and ground: Adopting no free sliding wall.

## 3.2 Calculation Results and Analysis

According to (Wang and Wang 2015), it can be seen that the SST  $k$ - $\omega$  shear stress transport model has better convergence than the BSL-RSM Reynolds stress model. Therefore, SST  $k$ - $\omega$  shear stress transport model has been chosen. Within the B type geomorphic wind field, the model was simulated under the 7 wind directions. The surface of the structure is divided into four regions, A, B, C and D. Each region is divided into 15 sub-regions, totaling 60 sub-regions, as shown in Figure 4. The average wind pressure coefficient of measuring points corresponding to the 60 partitions on the roof surface is also monitored.

D1	D2	D3	D4	D5	D6	D7	D8	D9	D10	D11	D12	D13	D14	D15
C1	C2	C3	C4	C5	C6	C7	C8	C9	C10	C11	C12	C13	C14	C15
B1	B2	B3	B4	B5	B6	B7	B8	B9	B10	B11	B12	B13	B14	B15
A1	A2	A3	A4	A5	A6	A7	A8	A9	A10	A11	A12	A13	A14	A15

Figure 4. Number of measuring points on the structure surface.

The model is a semi open membrane structure, with different wind pressure on the upper and lower surface of the structure, which is subject to the wind load. Therefore, after obtaining wind pressure on the upper and lower surface, the resultant force of the structure and the corresponding wind pressure coefficient after superposition are obtained by the block superposition treatment of the surface of the structure.

Take the  $90^\circ$  wind direction as an example, the average wind pressure coefficient and velocity streamline of the structure surface are analyzed (Figure 5 and 6). Because the central section of the windward of the structure is concave and it is a larger area, the impact and the stagnation point will occur when passing through the air. Thus, the maximum point of positive pressure is generated, which is concentrated in the middle of windward side, with the maximum positive pressure coefficient 1.10. When the airflow is impeded in the central section of the windward side, it begins climbing to the top and sides of the roof. When climbing to the ridge, the airflow separated apparently forming the tiny discrete high-speed vortex and falling off the back ridge, thus, generating great wind suction near the separation point. Therefore, from the lower to the upper edge of the roof, the average wind pressure coefficient decreases gradually. The positive pressure is gradually transformed to the negative pressure when the airflow nears the

ridge. The maximum negative pressure area is concentrated in the central of two wings of the ridge, with the maximum negative pressure coefficient -2.304.

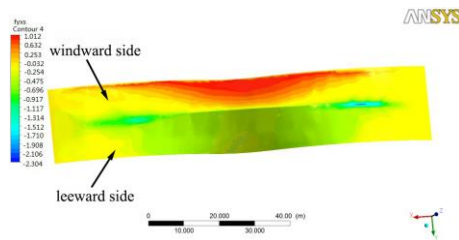


Figure 5. Average wind pressure coefficient (90°).

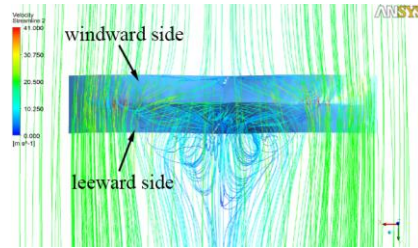


Figure 6. Velocity streamline.

Due to the adhesion and separation of airflow, greater suction is produced. The negative wind pressure in the middle part of leeward of the structure is smaller, and it increases with the extension to both sides. The negative pressure begins to decrease when it is 1/3 meter away from the edge of the wing, until reduced to the minimum at the edge of the wings. The negative pressure at the entire leeside is obviously smaller than that at the ridge.

The results show that the maximum wind pressure area on the windward side is concentrated on the areas of A8, A9 and A10 that are located in the middle part of the windward. And the average wind pressure coefficient of the three areas is between 0.75 and 1.25. The negative pressure area on the windward side is mainly concentrated on B1 and B2 that are located in the ends of the windward's two wings. The negative pressure area on the windward side is mainly concentrated on the areas of B1 and B2 that are located the ends of the windward's two wings. The maximum negative wind pressure on the leeside is mainly concentrated on the areas of C11 and C12 that are located in the ridge of the middle part of the two wings. And the average wind pressure coefficient of the two areas is between -1 and -2. The D area in the leeside is the least affected by the airflow and its average wind pressure coefficients are very small under the 7 wind directions.

To sum up, when the wind angles are between 60°-90°, the absolute value of the average wind pressure coefficient of the structure surface is larger, with wider distribution. The maximum positive and negative mean wind pressure coefficients have little difference, which shows that the structure is greatly influenced by the wind load in the range of the wind angle.

### 3.3 Shape Factor of Wind Load

The average wind pressure coefficient is converted into the wind load shape coefficients (Table 1), which is used as the load parameter of static analysis. The average wind pressure coefficient  $C_{pi}$  obtained from numerical wind tunnel simulation is reference to the wind pressure at 10m height. The shape coefficient of wind load  $\mu_{si}$  at different heights is corrected by the change of wind pressure height.

## 4 FIELD LOADING TEST

### 4.1 Loading Scheme

Adopting grading loading system, the loads from the first to third grade are 40%, 80%, and 100% respectively of the set load. Preloading is needed before test, and the load is 10% of set load.

After unloading, formal load starts (Wang *et al.* 2012). Each load should be stabilized for 30 minutes and then proceed to next level loading.

Table 1. Structural shape factor of wind load (90°).

Area	Factor	Area	Factor	Area	Factor	Area	Factor
A1	-0.270	B1	-0.213	C1	-0.157	D1	-0.199
A2	-0.235	B2	-0.194	C2	-0.180	D2	-0.201
A3	-0.213	B3	-0.180	C3	-0.314	D3	-0.219
A4	-0.128	B4	-0.156	C4	-0.583	D4	-0.449
A5	0.162	B5	-0.103	C5	-0.572	D5	-0.447
A6	0.270	B6	-0.054	C6	-0.574	D6	-0.448
A7	0.676	B7	-0.026	C7	-0.579	D7	-0.427
A8	1.080	B8	0.178	C8	-0.578	D8	-0.407
A9	1.082	B9	0.173	C9	-0.572	D9	-0.415
A10	0.276	B10	-0.009	C10	-0.570	D10	-0.446
A11	0.161	B11	-0.101	C11	-0.563	D11	-0.449
A12	-0.126	B12	-0.158	C12	-0.489	D12	-0.451
A13	-0.210	B13	-0.178	C13	-0.310	D13	-0.220
A14	-0.234	B14	-0.196	C14	-0.178	D14	-0.199
A15	-0.270	B15	-0.211	C15	-0.135	D15	-0.162

When loading, the tension of multiple cables simulates the multi-point loads on the structure under wind load. The test system consists of DH3816 static strain acquisition instrument, steel surface strain meter and strain gauge, adopting high precision total station to record the displacement in three directions of each measuring point. According to the simulation results of the numerical wind tunnel, the key parts of the structure are determined and arranging the measuring point. Considering the influence of wind speed at the test site, the real-time wind speed and direction are monitored by the wind speed indicator and wind direction indicator. The wind speed and wind direction data are used to convert the required tension, and the test load is adjusted in real time.

## 4.2 Test Results

**The first loading grade:** Start loading from the third group and stop loading when 40% of the set load is reached. The first group starts loading, when the loading reaches at 40% of the set load, stops loading. The second group starts loading, when the loading reaches at 40% of the set load, stops loading. Thus, the first-grade load ends. At this point, the stress value of each measuring point is -60~80MPa, and the overall structure is in an elastic state.

**The second loading grade:** Start loading from the second group and stop loading when 80% of the set load is reached. The third group starts loading, when the loading reaches at 80% of the set load, stops loading. The first group starts loading, when the loading reaches at 80% of the set load, stops loading. Thus, the second-grade load ends. The stress of the measuring point is -60~60MPa, and the number of the measuring points increases when the stress is -60MPa.

**The third group loading:** Start loading from the first group and stop loading when the set load is reached. The second group starts loading, and stops loading, when the reaching the set load. The third group starts loading and stops loading when reaching the set load. Thus, the third-grade load ends and all the process of loading is completed. At this point, the stress value of each measuring point is -120~20Mpa, and the stress of some measuring points increases obviously, with the maximum value close to -120MPa. The structure is still in an elastic state.

After all loading is finished, keep the loading steady for 30 minutes and then start unloading. After unloading, keep the structure steady for 60 minutes and then start measuring data. At this point, the stress of all the measuring points tends to zero, which shows that the structure in the whole experiment is in the elastic stress state fully.

## 5 CONCLUSIONS

In this paper, the toll station of *Liu Zhaike* expressway is taken as an example, the numerical simulation and field load test of the complex curved rectangular tube truss structure are carried out, and the main conclusions are drawn as follows:

When the wind direction is between  $60^\circ$  and  $90^\circ$ , the absolute value of the average wind pressure coefficient of the structure surface is greater, with a wider range of distribution.

During the test, the maximum stress is far less than the design strength of the component. After unloading, the stress and displacement of the structure can be restored to the initial state, indicating that the structure is working in an elastic state.

Under the asymmetric load working condition, the stress of some web member in the structure appears inverse phenomenon, which means the tension and compression state of the member is converted reciprocally. If the load increases to a certain value, it will lead to the destabilizing of the belly bar and affect the safety of the structure.

### Acknowledgments

The authors would like to thank the financial support from the National Natural Science Foundation of China (51778273).

### References

- Chen, B., Yang, Q., and Wu, Y., Multi-Objective Equivalent Static Wind Loads for Large-Span Structures (in Chinese), *China Civil Engineering Journal*, 43(3), 62-67, 2010.
- Li, X., Numerical Simulation Study of Wind Load on Structures Based on CFD (in Chinese), *Guangzhou: School of Civil Engineering and Transportation, South China University of Technology*, 2013.
- Ma, J., Zhou, D., and Li, H., Numerical Wind Tunnel Technique for The Wind Resistance Analysis of Long Span Spatial Structures (in Chinese), *Engineering Mechanics*, 7(24), 77-93, 2007.
- Pan, F., Refinement Theory of Random Wind-Induced Dynamic Response for Long-Span Roof Structures, (in Chinese), *Hangzhou: Institution of Architecture and Civil Engineering, Zhejiang University*, 2008.
- Shen, S., and Wu, Y., *Present Situation and Prospect of Wind Resistant Research on Long-Span Space Structures (in Chinese)*, in Proceedings of the 30th Anniversary of The General Assembly on Structural Wind Engineering Research in China, 94-103, China Civil Engineering Society, 2010.
- Wang, X., Li, Y., and Yang, W., Health Monitoring and Simulation Analysis Over Construction Loading Process for Long-Span Steel Structure (in Chinese), *Spatial Structures*, 18(4), 49-54, 2012.
- Wang, X., and Wang, X., Numerical Simulation of Wind Pressure Distribution on the Cantilever Steel Truss Roof Structure with Multi-Zigzag Plane Shape (in Chinese), *Spatial Structures*, 21(1), 26-33, 2015.
- Xiang, H., State of the Art and Prospect in Studies on Structural Wind Engineering (in Chinese), *Journal of Vibration Engineering*, 10(3), 258-263, 1997.
- Zhou, X., Gan, M., and Li, G., Grouping Response Method for Equivalent Static Wind Loads Based on a Modified LRC Method, *Earthquake Engineering and Engineering Vibration*, 11(1), 107-119, 2012.